



Deposited via The University of Sheffield.

White Rose Research Online URL for this paper:

<https://eprints.whiterose.ac.uk/id/eprint/75892/>

Monograph:

Edwards, J.B. (1974) Stability Problems in the Control of Multipass Processes. Research Report. ACSE Report 24 . Department of Control Engineering, University of Sheffield, Mappin Street, Sheffield

Reuse

Items deposited in White Rose Research Online are protected by copyright, with all rights reserved unless indicated otherwise. They may be downloaded and/or printed for private study, or other acts as permitted by national copyright laws. The publisher or other rights holders may allow further reproduction and re-use of the full text version. This is indicated by the licence information on the White Rose Research Online record for the item.

Takedown

If you consider content in White Rose Research Online to be in breach of UK law, please notify us by emailing eprints@whiterose.ac.uk including the URL of the record and the reason for the withdrawal request.

Department of Control Engineering

University of Sheffield

Research Report No. 24

Stability Problems in the Control of Multipass Processes

J. B. Edwards

April 1974

Stability Problems in the Control of Multipass Processes

J. B. Edwards

Abstract

The general characteristics of multipass processes are discussed and a method of process modelling is proposed based on the single independent variable : total distance passed. The stability of a number of such processes, including longwall coal-cutting, ploughing and metal-rolling is examined using this type of model analysed by the inverse Nyquist technique. Important stability problems, arising from the multipass nature of the processes, are exposed in all cases. Transport delays and resonance in the single-pass loops are shown to be particularly troublesome.

A general approach to the dynamic analysis of bidirectional systems is outlined using discrete time-series observation.

1. Symbols and Abbreviations

- a = state variable of coal cutter steering process, (tilt)
- E = matrix of face-length delay terms $\exp(-Ls)$, and zeros
- F_e = force applied by roll setting drive
- F_s = roll force applied to metal strip
- G = general symbol denoting open-loop transfer function
- $G_{1...4}$ = transfer-function matrices
- J = input variable to coal cutter steering process
- k_g = tilt gain of coal-cutter controller
- k_h = height gain of coal-cutter controller
- k_1 = gain of roll-positioning servomechanism
- k_2 = gain of stabilising feedback in this servo
- k_3 = gain of outer loop of gauge-control system
- k_4, k_5 = gain constants in rolling process
- ℓ = distance traversed by, or along, one pass
- L = pass length

- m = integer number of passes
- M = mass representing lumped inertia of roll servo system
- n = integer number of passes (even no. in section 5)
- p = Laplace operator with respect to time t
- r = gauge reduction factor
- R = transfer function of the operation: "record function and reverse its time sequence"
- R = matrix of transfer functions R, and zeros
- s = Laplace operator with respect to v' (and v where this denotes a variable distance)
- S = speed of pass (at output in the case of the rolling process)
- T , with various suffixes appended, denotes various process time-constants and delays
- u = vector of process inputs
- v' = variable denoting total distance passed
- v = as v', (except in section 5 where v denotes a particular value of v')
- X = displacement between process output sensor and process tool
- y = process output vector
- y = process output; coal thickness, distance between consecutive furrows, according to the process in question
- y_{ref} = reference value of y
- +y_i = input strip gauge
- +y_o = output strip gauge
- +y₁ = screw down displacement
- +y_{1d} = demanded y₁
- y_{oref} = reference value of y_o
- z = process disturbance
- λ₁ = stiffness of work rolls and their supports
- λ₂ = yield coefficient of metal strip

+These symbols are also used to represent the process variables normalised with respect to their time-varying references.

- Λ = composite stiffness of strip and rolls
 ζ = damping ratio
 ω_0 = undamped natural frequency

2. Introduction

The rolling of metal strip, the ploughing of agricultural land, the longwall cutting of coal and a variety of machining operations are processes which are similar in that the material, or workpiece, involved is processed by a sequence of passes of the processing tool. During each pass relative motion occurs between tool and workpiece and it is unimportant in the dynamic analysis of such processes which of these two is the stationary member and which is moving. The output vector function generated during pass n may be denoted by $\underline{y}(n, \ell)$, where ℓ is the distance traversed along the pass whose total length is, say, L . (In some processes, such as rolling, $L = L(n)$ and will vary between passes, but more often it is sensibly constant). This output vector function acts as a forcing-function on the next pass, number $n+1$, and thus contributes towards the new output $\underline{y}(n+1, \ell)$. As illustrated diagrammatically in figure 1, multipass processes may be unidirectional or bidirectional. In the former case during processing, the relative motion between tool and material takes place in one direction only. In bidirectional processes the material is processed in each direction alternately.

Figure 2 shows in block-diagram form a general dynamic representation of a multipass process. The inter-pass feedback is shown acting via a transfer function matrix $\underline{E}(s)$, whose non-zero elements are delay terms, $\exp(-Ls)$, in the case of unidirectional processes, or via the matrix $\underline{R}(s)$ in the case of bidirectional processes. The non-zero elements $R(s)$ of this latter matrix are dynamic operators of a more complex type describing the process of function recording and subsequent readout in reverse time-sequence. The process $R(s)$ is illustrated graphically in figure 3. Bidirectional processes are considered in section 5, up to which point attention is confined to the

more readily analysed unidirectional type.

As indicated in figure 2, multipass processes may, in principle, be controlled on pass $n+1$ by feedback of either $\underline{y}(n+1, \ell)$ or $\underline{y}(n, \ell)$. Earlier output vector functions or a combination of several may conceivably be used for control of the process. Physical restrictions on the siting of some of the necessary transducers usually demand that, in extracting present-pass information, some delay in sensing is unavoidable such that, at instant $n+1, \ell$, only the signal $\underline{y}(n+1, \ell-X)$ is accessible, where X is the sensor/tool separation. The accessibility of $\underline{y}(n, \ell)$ for control purposes may depend, as in the case of coal cutting¹, on the availability of digital computer storage. The controller designer may therefore have to cope with certain elements within the transfer function matrices $\underline{G}_3(s)$ and $\underline{G}_3'(s)$, (figure 2), which are prespecified.

It is frequently the case that automatically-controlled multipass processes appear perfectly stable on a single-pass assessment but are never-the-less highly unstable over a sequence of passes. Such instability, when present, is predictable analytically if the process variables are expressed as functions of the single coordinate v , [$= (n-1)L + \ell$], = total pass distance up to the point n, ℓ , {i.e. $\underline{y}(n, \ell)$ becomes $\underline{y}(v)$ }, and by taking Laplace transforms of the system with respect to v . The unidirectional coal-cutter steering process, for instance, is governed by the equations

$$y(v) = y(v-L) + a(v-L) + J(v-L) \quad (1)$$

$$\text{and } a(v) = a(v-L) + J(v-L) \quad (2)$$

and the control algorithm in current use is

$$J(v-L) = k_h [y_{\text{ref}} - y(v-X)] - k_g a(v-L) \quad (3)$$

y and a being the process states and J the control. Control law 3 uses previous-pass values of a and present-pass values of y , though delayed by sensor displacement, X . If, for convenience only, gain k_g is set to unity, the system reduces to the form shown in figure 4, and its open-loop transfer-function becomes

$$G(s) = \frac{k_h \exp(-Xs)}{\{1 - \exp(-Ls)\}} \quad (4)$$

the inverse Nyquist plot of which takes the form of figure 5. The process is clearly unstable for all practical values of X , ($X \ll L$), since the critical point is encircled for all gains k_h , even though the single-pass loop may be stabilised merely by setting k_h less than unity. As shown in earlier work¹ by the authors, the process may only be stabilised by extending X artificially to equal L , but this requires storage facilities not available to current analogue controllers.

In the present paper the method of modelling, (in terms of v), and of analysis, (in terms of the inverse Nyquist locus), developed by the authors¹ for the coal-cutter are applied to a number of other multipass processes and developed for general application.

3. Self-Steered Tractors

Figure 6 shows the important process variables defining the state of this system, the object of which is to maintain straight furrows, parallel to some datum line, and equi-spaced at intervals y_{ref} . When no buried guide-wires exist, some form of mechanical or electro/optical sensor is employed to measure the error signal, $y_e(v)$, in the displacement between consecutive furrows n and $n-1$, the present furrow being the n th. The control systems, described in detail by Hilton and Chestney² and by Julian³, are of relatively-high order and contain some mild non-linearities. Fundamentally, however, the error signal is amplified and integrated through the steering action of the front wheels, at which point the disturbances $z(v)$ act upon the process. For present purposes a second-order model* of this single-pass loop is employed, described by the equations

*Simulation and inverse Nyquist loci based on the full single-pass dynamics yield the same general conclusions as predictions based on this model.

$$\ddot{y}(v) + \ddot{z}(v) = y_e(v) \cdot \omega_o^2 + \{\dot{y}(v) + \dot{z}(v)\} 2\zeta\omega_o \quad (5)$$

$$\text{and } y_e(v) = y_{\text{ref}} - y(v) \quad (6)$$

where ω_o and ζ are constants if constant speed is assumed. However, as is obvious from figure 6, the system output $y(v)$ contributes towards the next disturbance $z(v+L)$ in the manner:

$$z(v+L) = y(v) + z(v) \quad (7)$$

and, likewise,

$$z(v) = y(v-L) + z(v-L) \quad (8)$$

[This interaction between passes occurs purely through the controller, attention here being confined to the currently popular "out of furrow ploughing". Further interactions occur within the process itself if ploughing takes place with one back wheel in the previous furrow].

Equations 5, 6 and 8 yield a block diagram for the unidirectional multi-pass process of the form shown in figure 7 and its stability can be determined by examination of the open-loop transfer function

$$G(s) = \frac{\omega_o^2 \exp(-Ls)}{\omega_o^2 + 2\zeta\omega_o s + s^2} \quad (9)$$

The system parameter, ω_o , represents the undamped natural frequency of the single-pass loop and will be of such a magnitude that:

$$\omega_o \gg 1/L \quad (10)$$

The inverse Nyquist locus for $s = j\omega$, is therefore a spiral orbiting the origin of $G^{-1}(s)$ counterclockwise and making approximately one revolution for a frequency change, $\Delta\omega = 2\pi/L$. If the single-pass loop is at all oscillatory, or more precisely if $\zeta < 0.707$ then the encirclements of the critical point $-1, j0$ for ω finite, will be more than compensated by the infinite radius clockwise orbits* described by $G^{-1}(s)$ when s is set to $R_a \exp(j\theta)$, where

* For the complete inverse Nyquist stability criterion references 1 and 4 should be consulted.

$R_a \rightarrow \infty$ and $\pi/2 > \theta > -\pi/2$, and under such circumstances the multipass system will be unstable.

The simulated system response to a step disturbance in the first furrow is shown in figure 8, for the case of $\zeta = 0.5$, and clearly demonstrates the predicted instability. If, however, the single-pass loop is overdamped the responses take on an approximately exponential form of progressively increasing time-constant, ultimately becoming straight, but no longer parallel to the original datum. This confirms Hilton's observations² of the behaviour of an actual tractor whose servo system was presumably overdamped. Unlike the coal-cutter problem discussed earlier, multipass instability of the self-steered tractor, whilst being a potential danger in view of the speed-dependence of, ζ , is fairly readily avoided in this case.

The basic causes of instability would seem to be different in the two problems. In tractor steering the instability can perhaps be loosely explained in terms of repeated excitation of the single-pass resonance. In coal-cutter steering, the sensor delay X is the root cause of instability but its effects are too profound for convincing qualitative explanation.

The two processes so far considered are similar, however, in as much as the multipass feedback re-enters the process at its output via a non-dynamic transmittance of unit gain, (see equations 1 and 8). It is important at this stage therefore to examine the behaviour of a multipass process in which the transfer function matrix $G_2(s)$, (figure 2), includes other than mere unit-gain terms. Metal rolling is such a process, interpass feedback resulting from the yield of the workrolls and their supports, which is clearly dependent on the gauge of the incoming strip, i.e. on the previous output gauge.

4. Metal Rolling

Since the practical object of the paper is to assess whether or not multipass instability is a serious risk worthy of deeper investigation attention is here restricted to multipass rolling through a single stand, (a process often

described as "cogging"). In practice this method of rolling is generally restricted to billet-processing rather than strip-processing and it is often only the latter process which is subject to tight tolerances. However, multipass strip-rolling through a single stand could be attractive economically where space restrictions preclude the use of several stands in tandem. This introductory study of the control problems associated with multipass rolling could therefore have more than mere academic relevance. In this section the unidirectional process is analysed whereas cogging is more conveniently accomplished bidirectionally in practice. The stability conclusions are virtually unaffected, however, as will be demonstrated in section 5.

4.1 Process Model

Figure 9 illustrates the physical basis of the model to be adopted and shows strip entering and leaving the rolls at a gauge $y_i(n,t)$ and $y_o(n,t)$ respectively. The gauge is adjusted by indirect manipulation of the measurable screwdown displacement $y_1(n,t)$ which is set to a demand $y_{1d}(n,t)$ with feedback control which sets the force $F_e(n,t)$ applied by the screwdown drive. The total system inertia is here lumped at the drive and represented by the mass M shown in figure 9. The spring of stiffness λ_1 represents the yield of the work-rolls etc. It is assumed, for a particular steel, that the vertical roll force $F_s(n,t)$ is proportional to the reduction $y_i(n,t) - y_o(n,t)$. The model is therefore described by the equations:

$$F_s(n,t) = \lambda_1 \{y_1(n,t) + y_o(n,t)\} \quad (11)$$

$$F_s(n,t) = \lambda_2 \{y_i(n,t) - y_o(n,t)\} \quad (12)$$

$$F_e(n,t) = F_s(n,t) + M \ddot{y}_1(n,t) \quad (13)$$

where F_e is set by proportional plus derivative servo-action, according to:

$$F_e(n,t) = k_1 \{y_{1d}(n,t) - y_1(n,t)\} - k_2 \dot{y}_1(n,t) \quad (14)$$

and where the demand y_{1d} is calculated by an outer gauge-control loop incorporating a displaced sensor thus:

$$y_{1d}(n,t) = -k_3 \{y_{oref}(n) - y_o(n,t-T)\} \quad (15)$$

, T being the transport delay in sensing the output gauge.

Now the gauge reference y_{oref} , though constant for one particular pass, is reduced progressively between passes according to, say,

$$y_{oref}(n) = r \cdot y_{oref}(n-1) \quad (16)$$

where

$$0 < r < 1.0 \quad (17)$$

If all the process variables are normalised with respect to the current gauge reference but denoted by the same symbols as previously, (e.g. if $y_o(n,t)/y_{oref}(n)$ is now denoted by $y_o(n,t)$), then the process model shown in figure 10, can be derived, clearly showing the non-unity gain of the inter-pass feedback and the dynamic terms present. The parameter Λ in figure 10 is the composite stiffness of the work-rolls and strip and is given by

$$\Lambda = \lambda_1 \lambda_2 / (\lambda_1 + \lambda_2) \quad (18)$$

and the natural frequency, ω_o , and damping ratio, ζ , of the single-pass system, (roll-setting servo), are given by

$$\begin{aligned} \omega_o^2 &= (\Lambda + k_1)/M \\ \text{and } 2\zeta\omega_o &= k_2/M \end{aligned} \quad (19)$$

4.2 Normalisation of the Distance Base

The Laplace operator, p , in figure 10 is taken with respect to time, t , but, unfortunately, a simple time-base is not strictly appropriate to the performance analysis of this type of process because of speed-changes between consecutive passes. Nor does absolute distance provide a correct basis due to the progressive lengthening of the pass which is governed by the equation:

$$L(n) = L(n-1)/r \quad (20)$$

if a constant width of strip is maintained. In fact, any particular elementary section of the strip located at some distance $\ell(n-1)$ from the end of the strip on pass $n-1$ will, on this assumption, be located at $\ell(n)$ on pass n , where

$$\ell(n) = \ell(n-1)r \quad (21)$$

Now process stability should be assessed on whether or not oscillations in the relative gauge* of any particular elementary section of the strip converge or diverge as n increases. For the analysis of stability, or general dynamic behaviour therefore, it is preferable to regard the strip-length as fixed at $L(1)$, ($=L$), such that the arbitrary strip section under observation remains at a distance $\ell(1)$, ($=\ell$), from the end of the pass. This, of course, demands that truly fixed horizontal distances, such as the sensor displacement X , must now be considered as reducing as n increases, according to

$$X(n) = X(n-1)r = X r^{n-1} \quad (22)$$

The truly time-based dynamic parameters in figure 10 would, on this basis, require modification as follows

$$\omega_o(n) = \frac{\omega_o}{S(n) r^{n-1}} \quad (23)$$

where $\omega_o(n)$ is the undamped natural frequency of the roll-setting servo with respect to ℓ , and $S(n)$ denotes the output speed on pass n . Furthermore, since it is likely that the speed will be increased as n increases, it may be reasonably taken that

$$S(n) = \frac{S(n-1)}{r} = \frac{S(1)}{r^{n-1}} \quad (24)$$

so that, from equations 23 and 24 we have

* relative gauge = the strip gauge normalised with respect to the current reference gauge.

$$\omega_o(n) = \frac{\omega_o}{S(1)} = \text{a constant} \quad (25)$$

To this realistic basis, therefore, the process dynamic coefficients all become constant, or nearly so, with the exception of the sensor delay distance, $X(n)$.

4.3 Determination of System Stability

It is convenient and illuminating to consider first of all the performance of the process in the absence of all dynamic terms other than the two delays which are fundamental system constituents. On making this simplification, the process block diagram reduces to the form shown in figure 11, the open-loop transfer function of which is, for the n th pass,

$$G(s) = \frac{k_4 \exp\{-X(n)s\}}{1 - k_5 \exp(-Ls)} \quad (26)$$

where $k_4 = \frac{k_1 k_3 \Lambda}{(\Lambda + k_1) \lambda_2}$ (27)

and $k_5 = \frac{1}{r} \frac{\Lambda}{\lambda_1} + \frac{\Lambda^2}{\lambda_2 (\Lambda + k_1)}$ (28)

Apart from the time-varying sensor delay, the chief difference between the fundamental multipass dynamics of the coal cutter, (equation 4 and figure 4), and this rolling process, (equation 26 and figure 11), is, as expected at the outset, the existence of the non-unity gain term, k_5 , in the interpass-feedback loop of the latter. This gain has a readily-appreciated physical significance since, if it is assumed that the strip is relatively "soft" and the rolls relatively "hard", i.e. if

$$\lambda_1 \gg \lambda_2$$

then $k_5 \approx \frac{1}{r} \frac{\lambda_2}{\lambda_1} \left(1 + \frac{\lambda_1}{k_1}\right)$ (29)

and $k_4 \approx k_3$ (30)

where k_1 , previously defined, is the stiffness of the roll-setting servo, and k_3 is the gain of the outer gauge control loop. Equations 29 & 30 also assume that

$$k_1 \gg \lambda_2 .$$

Clearly from equations 26 and 29, if the steel is very soft such that roll-yield is completely negligible, k_5 tends to zero and the process dynamics reduce to those of merely the single-pass loop, as would be expected. Assuming that roll-yield is not negligible however, then k_5 will be significant, increasing with increasing reduction rate and with the ratio of the roll to servo stiffness, (λ_1/k_1) . Values of k_5 approaching, or perhaps even exceeding, unity could well be approached in some cases therefore, despite λ_2/λ_1 itself being fairly small.

Ignoring for the moment the fact that $X(n)$ is time-varying, figure 12 shows the inverse Nyquist plot of the system for the moderate value of $k_5 = 0.5$, (obtained, for instance, with $r = 0.8$, equal λ_1 and k_1 and a λ_2/λ_1 ratio of 0.20). Clearly, if $k_5 < 1.0$, unlike the coal-cutter case, there exists a stable central region of the $G^{-1}(s)$ plane in which to locate the critical point which is achieved by ensuring that

$$k_4 < 1 - k_5 \tag{31}$$

For single pass stability, of course, it is merely necessary that

$$k_4 < 1.0 \tag{32}$$

With k_4 adjusted to satisfy the multipass stability condition (31), the clockwise and counterclockwise encirclements of the critical point clearly counterbalance. Stability will, however, be achieved at the expense of a very low system gain and, if $k_5 > 1.0$, then stability is unachievable if the sensor is located behind the stand as assumed.

With the aid of an appropriate computer-aided frequency-response display package, the dynamic terms so far neglected can be included fairly readily, if

equation 24 holds), to produce inverse Nyquist loci of the complete process and scope does exist, with $k_5 < 1.0$, to manipulate the parameters of these terms to obtain stability not entirely at the expense of d.c. gain. It is essential to include the interpass feedback effect, however, since, with or without the inclusion of servo dynamics, single pass stability is no guarantee of multipass stability.

Inclusion of the time-variation of the sensor delay, $X(n)$, in analytical studies has yet to be investigated by the author, and this would seem to be a profitable study since simulation reveals that with values of r of the order of 0.8, although the process oscillates considerably, the oscillation amplitude does not grow so drastically as in the fixed delay problem.

5. Bidirectional Systems

Having revealed complete or potential instability in all the unidirectional processes considered so far, it is important at this stage to investigate whether or not bidirectional operation of the processes provides a cure for this instability. As illustrated in figure 2, a change from unidirectional to bidirectional working involves merely the substitution of the matrix $\underline{R}(s)$ for $\underline{E}(s)$ in the interpass feedback loop. The operation $R(s)$, (which constitutes the non-zero elements of $\underline{R}(s)$), is, however, much more complicated than the simple delay terms, $\exp(-Ls)$, already encountered in unidirectional processes. This operation is now considered in more detail.

5.1 Nature of the Transfer-Function of the "Record and Reverse" Process

The input/output relationship for this process, R , has already been illustrated in the time-, or more precisely distance-domain, in figure 3, which shows the process variable generated during pass n being stored as an entire function of distance and subsequently reappearing at the output of R in reverse time-sequence, during pass $n+1$. If the input $\theta_1(v')$ to the process R were, in fact, a unit impulse applied at instant, (n, ℓ) , then

$$\theta_1(v') = \delta(v'-v) \quad (33)$$

where v' denotes the general variable = cumulative pass distance, and v denotes its particular value at the instant, (n, ℓ) . The resulting output of R is given by

$$\theta_0(v') = \delta(v' - v - 2\ell) \quad (34)$$

Now as reference to figure 1b shows, ℓ and v are related by:

$$\ell = nL - v \quad (35)$$

and hence the unit impulse response of the process R is given by

$$\theta_0(v') = \delta\{v' - (2nL-v)\} , \quad (n-1)L < v < nL \quad (36)$$

Taking the Laplace transform of this response with respect to the variable v' yields the transfer-function of the record and reverse process, R , which is clearly distance-dependent and given by

$$R(s, v) = \exp\{-(2nL - v)s\} , \quad (n-1)L < v < nL \quad (37)$$

5.2 The Bidirectional Process Output as a Discrete Time-, (Distance-), Series

The transfer-function $R(s, v)$ is of no immediate value in the determination of the overall system stability since it would be meaningless to substitute any single value of v in equation 37 due to the very large variation of v over only a few passes of the process. This turns out not to be a serious limitation, however, since deeper consideration of the process reveals that the process vector used for stability assessment should not be the continuous function vector $\underline{y}(v')$ but the discrete time-series, (or more precisely, "discrete distance-series"), $\underline{y}(nL-\ell) + \underline{y}(nL+\ell)$ taken over all even values of n for a particular arbitrary station, ℓ , measured from one end of the pass. Figure 1b shows a sequence of such stations^{*} diagrammatically. Confining attention to

* All odd values of n could be used as an alternative but the distance ℓ in figure 1b would then need redefining from the r.h.s. of the diagram.

these stations only, v is restricted to the values given by

$$v = 2mL - \ell \quad \text{and} \quad v = 2mL + \ell \quad (38)$$

where m is any integer.

From equation 37 therefore, we have that

$$R(s, v) = \exp(-\ell s) , \quad v = 2mL - \ell \quad (39)$$

and
$$R(s, v) = \exp[-(L - \ell)s] , \quad v = 2mL + \ell \quad (30)$$

The bidirectional output sequences $\underline{y}(2mL - \ell)$ and $\underline{y}(2mL + \ell)$ may therefore be regarded as the outputs of two equivalent unidirectional processes of pass-length ℓ and $L - \ell$ respectively, the former sampled at instants $v = 2mL - \ell$ and the latter at $v = 2mL + \ell$.

5.3 Stability of the Bidirectional, Present-Pass Controlled Coal-Cutter

Applying the foregoing concepts to the coal-cutting process described by equations 1 to 3, yields a bidirectional system block-diagram shown in figure 13, which produces as output the time-series, y_ℓ , defined by

$$y_\ell = y(2mL - \ell) + y(2mL + \ell) \quad (41)$$

The two sub-processes of figure 13 are clearly identical to the unidirectional process of figure 4 apart from the delay distances in the interpass feedback loops. Now if either of these subprocesses is unstable then sequence y_ℓ will be unstable since, in general, there will be no synchronism between the operation of the samplers and the oscillations of the sub-processes. Since it was concluded that the unidirectional process, (figure 4), would be unstable for all $X < L$, the bidirectional subprocesses will likewise be unstable for most values of ℓ . In fact it would appear that, for all multipass processes involving present-pass sensor delays X , ($\ll L$), then, if the process is unstable on unidirectional operation, it will also be unstable when operated bidirectionally, for most values of ℓ .

The predicted instability of the vertical steering system of the bidirectional coal cutter is here confirmed by figure 14 which illustrates the

transient response to a step fault in the coal/stone interface. A sensor time-constant T_2 and an actuator time-constant T_3 have here been included in the system dynamics but their inclusion has no bearing on the analytical stability conclusions.

6. Conclusions

A method of modelling multipass processes in terms of a single independent spatial variable has been presented and successfully applied to the processes of longwall coal-cutting, ploughing and metal rolling. The inverse Nyquist technique has in all cases predicted total or potential instability arising from either repeated excitation of the single-pass resonance or from the profound effects of the output sensor delay, both of which should therefore be avoided in such processes.

The stability of bidirectional processes should be assessed by observation of the discrete time-series output of the process at fixed distances from one end of the pass, (or at fixed relative distances in the case of variable pass-length processes). Such an approach reduces the bidirectional process to two repetatively-sampled unidirectional processes. Unidirectional instability would therefore imply bidirectional instability.

The effective time-variation in the output sensor delay in processes of varying pass length is an area for worthwhile analytical study in the future. Other multipass systems such as many machining operations and perhaps television signal processing should also profit from investigation on the lines here indicated.

7. References

- (1) Edwards, J.B. and Bogdadi, W.A., "Progress in the Design and Development of Automatic Control Systems for the Vertical Steering of Coal Cutters", Proc.I.E.E., (1973), Vol. , No. , pp.

- (2) Hilton, D.J. and Chestney, A.A.W., "Low-Cost Self Steering Devices for Out-of-furrow Ploughing", The Agricultural Engineer, Autumn Edition, 1973, pp.102-106.
- (3) Julian, A.P., "Design and Performance of a Steering Control System for Agricultural Tractors", J. Agric. Engng. Res. (1971), 16(3), 324-336.
- (4) Shinnars, S.M., "Control System Design", Wiley, New York, 1964, 523pp.

Fig. 2. Block Diagram of General Multipass Process

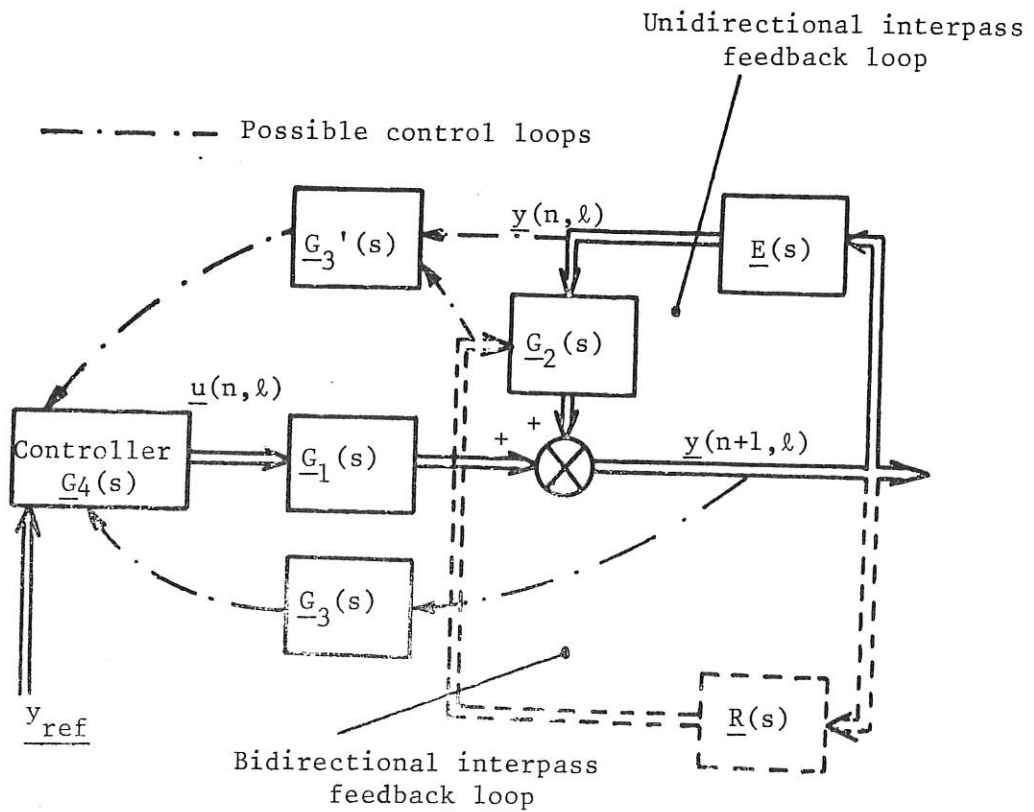


Fig. 3. Illustrating the "Record & Reverse" Process

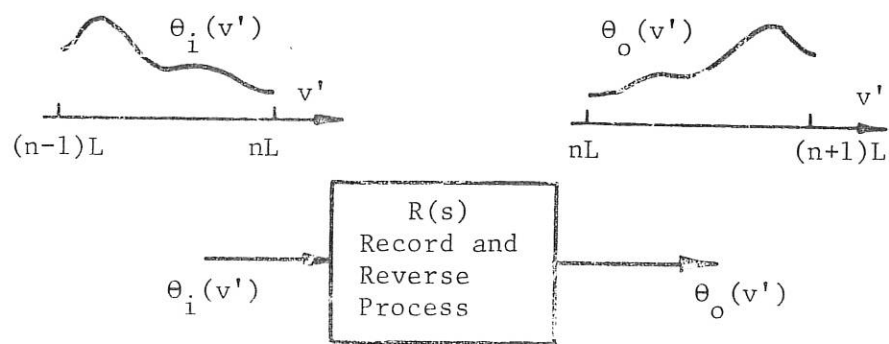


Fig. 4. Coal Cutter Steering System - Block Diagram

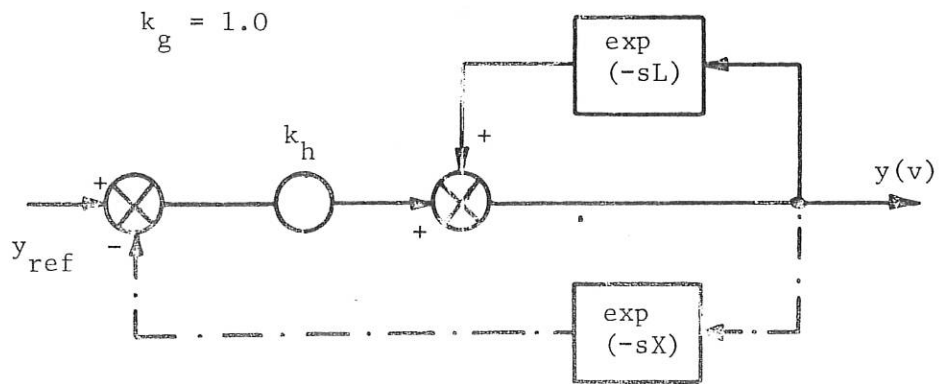


Fig. 5. Inverse Nyquist Diagram for Coal Cutting Process

$12X = L$

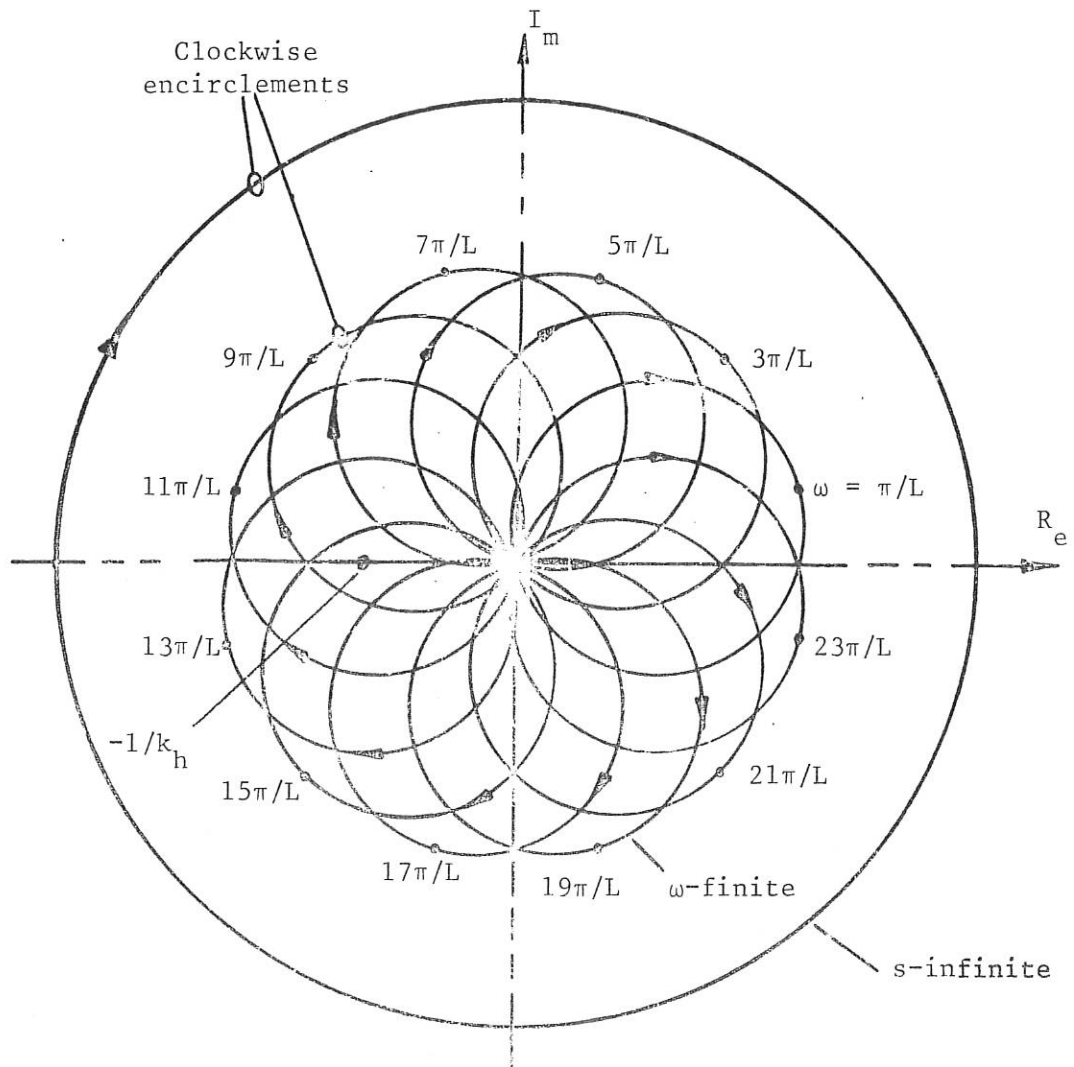


Fig. 6. Illustrating Main Variables in Tractor Steering

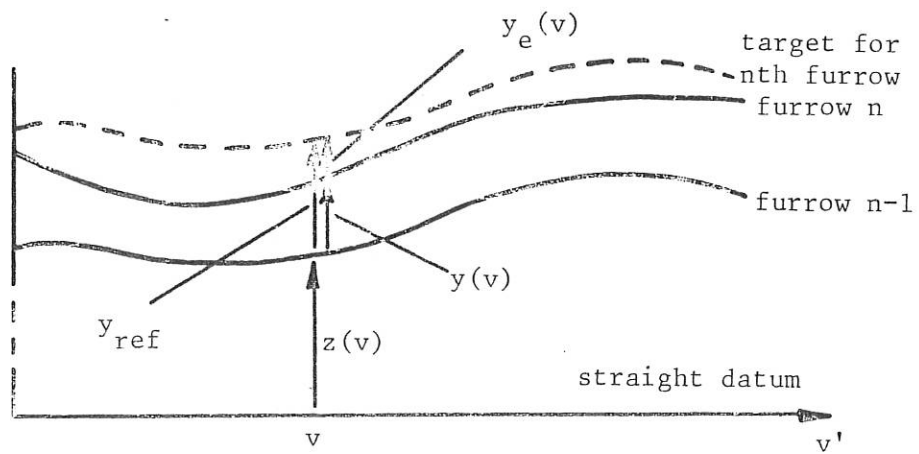


Fig. 7. Block Diagram for Self Steered Tractor

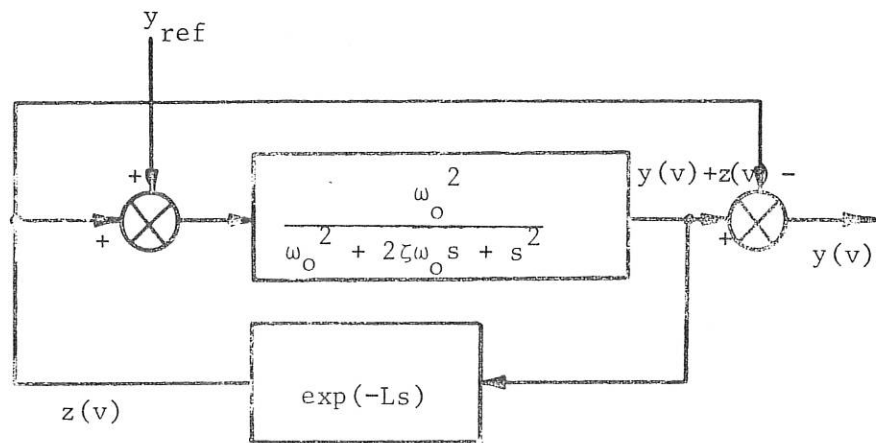


Fig. 8. Computed Response of Self Steered Tractor
to a Step in the First Furrow

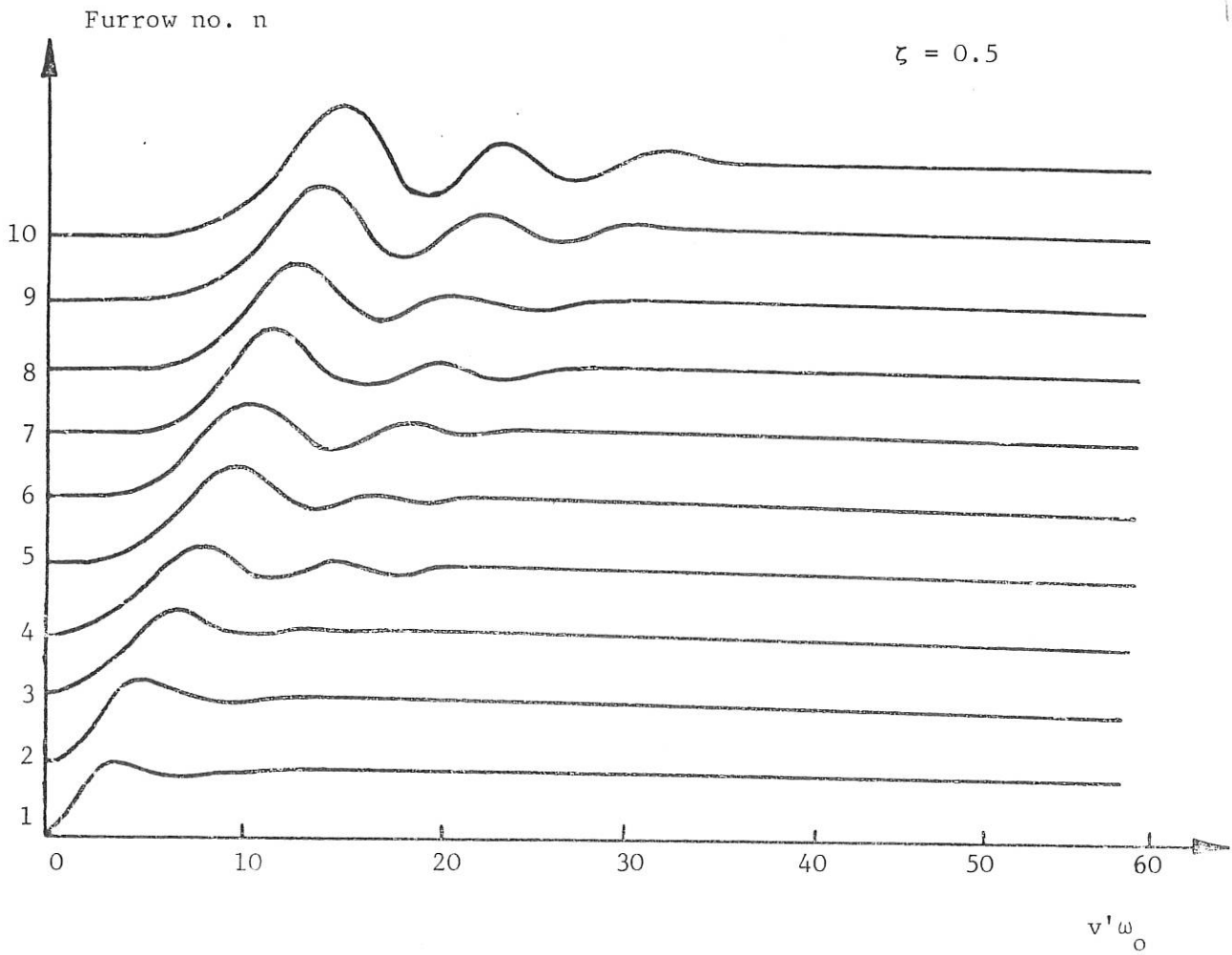


Fig. 9. Showing Physical Basis of Rolling Process Model

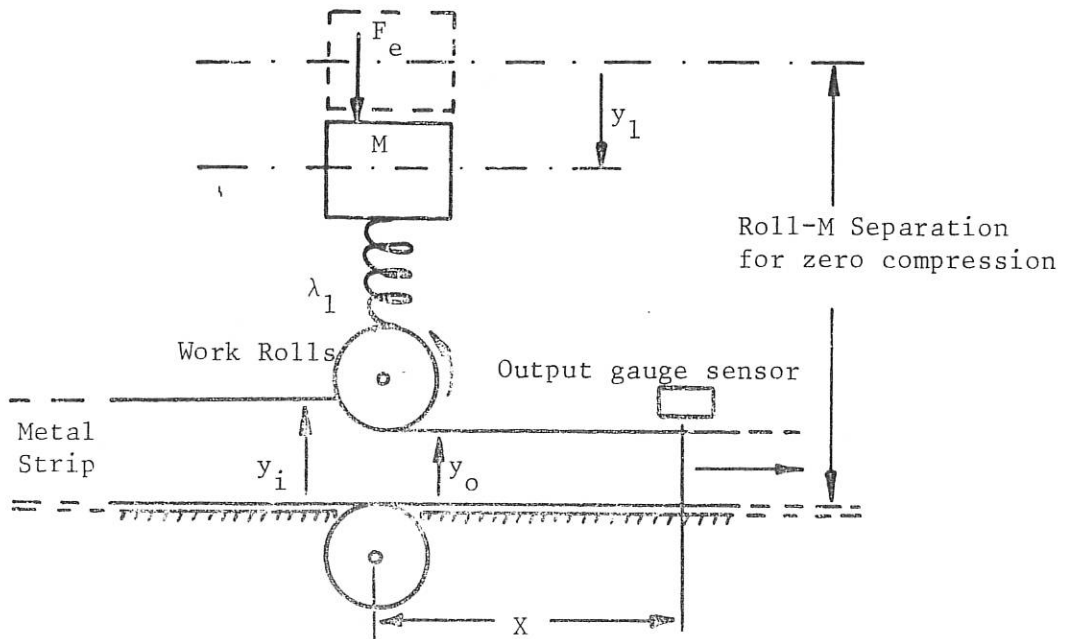


Fig. 10. Block Diagram Representation
of Rolling Process Dynamics

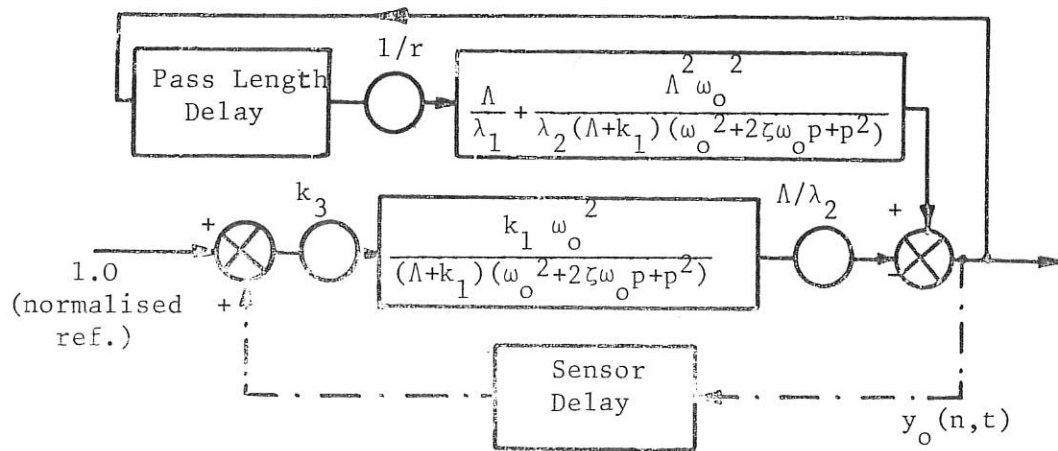


Fig. 11. Simplified Block Diagram of Rolling Process

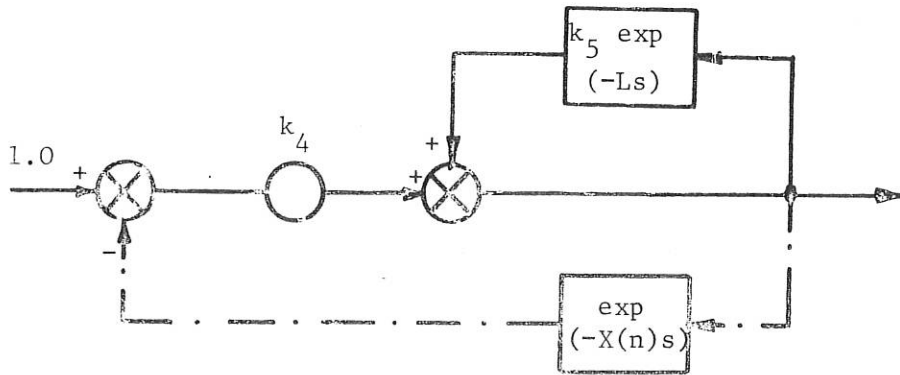
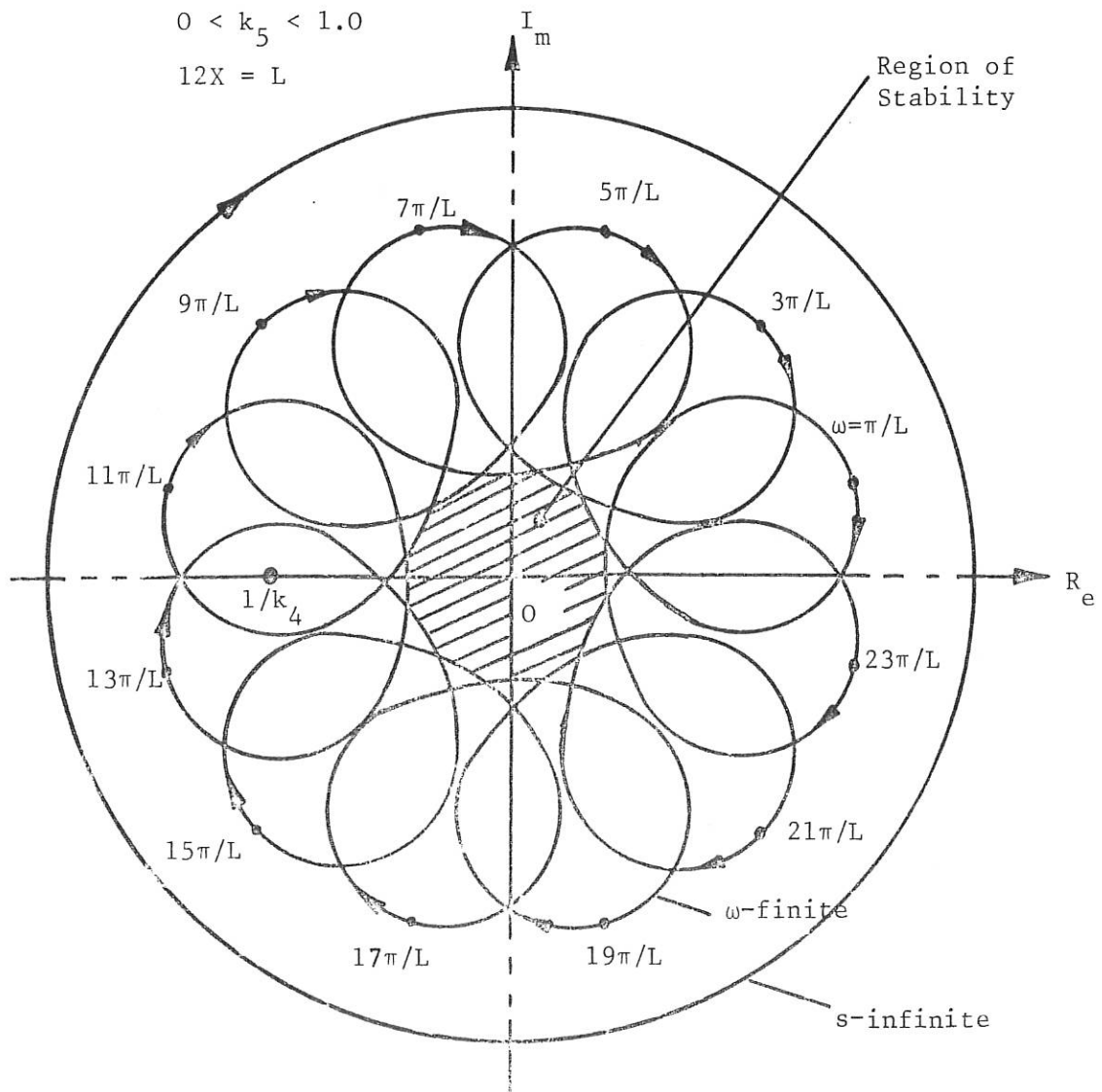


Fig. 12. Inverse Nyquist Diagram for Rolling Process



$S = 3.60 \text{ m/min}$ $T_2 = 10 \text{ sec.}$
 $k_h = 0.8$ $T_3 = 2.75 \text{ sec.}$
 $k_g = 1.0$ $X = 1.25 \text{ m.}$

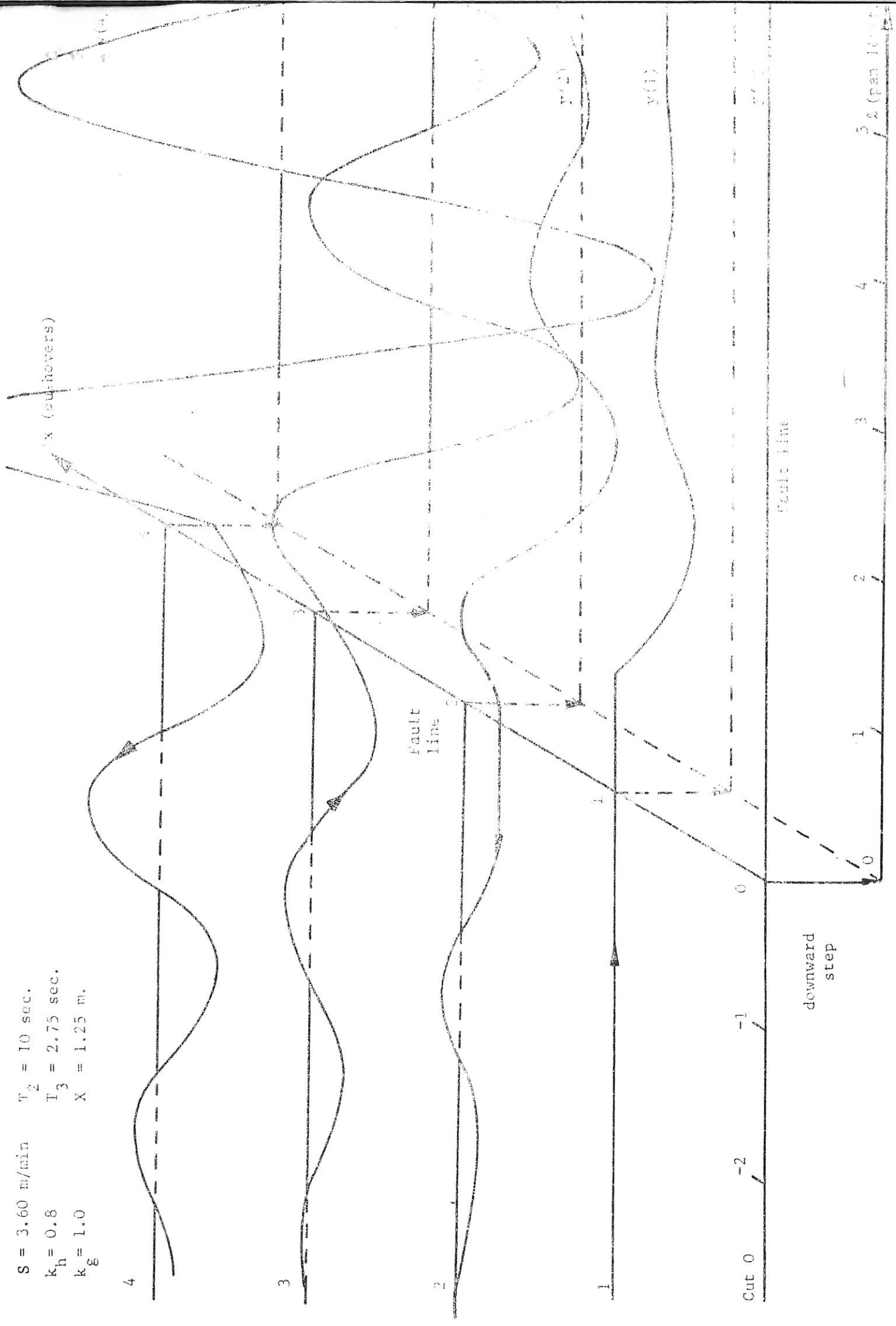


Fig. 14. Computed Response of a Bidirectional Coal Cutter to a Step Fault (Analog System)